Thermal transport in (Y,Gd)Ba$_2$(Cu$_{1-x}$Mn$_x$)$_3$O$_{7-\delta}$ for $x \leq 0.02$

Thermal transport in (Y, Gd)Ba$_2$(Cu$_{1-x}$Mn$_x$)$_3$O$_{7-\delta}$ for $x \leqslant 0.02$

Bhasker Gahtori[1,2]**, Ratan Lal**[1]**, S K Agarwal**[1,5]**, M A H Ahsan**[2]**, Ashok Rao**[3]**, Y F Lin**[4]**, K M Sivakumar**[4] **and Y-K Kuo**[4]

[1] Superconductivity and Cryogenics Division, National Physical Laboratory, Dr K S Krishnan Road, New Delhi-110012, India
[2] Department of Physics, Jamia Millia Islamia, New Delhi-110025, India
[3] Department of Physics, Mainpal Institute of Technology, Manipal-576104, India
[4] Department of Physics, National Dong-Hwa University, Hualien 974, Taiwan

E-mail: prof.agarwal@gmail.com

Abstract
Thermal conductivity $\kappa(T)$ and thermoelectric power $S(T)$ studies on (Y, Gd)Ba$_2$(Cu$_{1-x}$Mn$_x$)$_3$O$_{7-\delta}$ ($x \leqslant 0.02$) superconductors are presented here. Thermal conductivity for all the samples exhibits a hump below the superconducting transition temperature T_c. The peak height of the hump decreases with the Mn content in both the Y- and Gd-based systems, barring GdBa$_2$(Cu$_{0.99}$Mn$_{0.01}$)$_3$O$_{7-\delta}$. The peak height reduction in the Gd-based cuprates is much faster ($\sim$one fourth) compared to the Y-based samples. The thermoelectric power (TEP) of the Y-based samples for $x \leqslant 0.0075$ is electron-like (up to $\sim$140 K) whereas it turns to hole-like even at $x = 0.005$ for the Gd-based system. On the basis of the structure of the thermal conductivity hump, and of the electron- or hole-like nature of the thermopower, it has been argued that, in the Y-based system up to $x = 0.0075$, Mn produces qualitatively the same effect as Gd in the Gd-based system. An analysis of the thermal conductivity data in terms of lattice theory, and the TEP data in terms of a narrow-band picture, has been made to invoke the role of Mn in these systems. Boundary scattering, point defects and sheet-like faults (from $\kappa(T)$ data analysis) and chemical potential (from $S(T)$ data analysis) support different roles of Mn for $x \leqslant 0.0075$ and $x > 0.0075$.

1. Introduction

It is well established that partial substitution in cuprate superconductors in general leads to a change in the various properties of the pristine system [1–13]. Following such a

---

[5] Author to whom any correspondence should be addressed.

route the practical applicability of the material may also be greatly enhanced. As far as cuprate superconductors are concerned, relatively little work seems to have been done on Mn substitution, possibly due to its small solubility [1–7]. However, Mn doping is of great physical significance from the theoretical point of view due to some common features between the various transition metal ions. Interestingly, the transition temperature T_c of the Mn-doped (at Cu sites) $YBa_2Cu_3O_{7-\delta}$ (Y-123) system is only slightly affected by the Mn content [1, 2, 6, 7] unlike in the $GdBa_2Cu_3O_{7-\delta}$ (Gd-123) system [3]. Regarding the thermal behaviour of $YBa_2Cu_3O_{7-\delta}$ with other dopants at Cu sites, Loram *et al* [14] have studied the specific heat of Co-doped $YBa_2Cu_3O_{7-\delta}$, while Sisson *et al* [15] have studied the specific heat of the Zn-doped $YBa_2Cu_3O_{7-\delta}$ system. The thermoelectric power of Zn-, Pr- and Ca-doped Y- or Gd-based 123 systems has also been investigated [8–10]. Suleiman *et al* [11], Houssa *et al* [12], and Williams *et al* [13] have made studies of the thermal conductivity of the $YBa_2Cu_3O_{7-\delta}$ system by taking Co, Zn and Yb, Dy and/or Sr dopants, respectively. There are, however, only a few reports on thermal measurements of the Mn-doped $YBa_2Cu_3O_{7-\delta}$ system [3, 5, 7]. In particular, Gasumyants *et al* [5] and Samuel *et al* [7] have made a study of the thermoelectric power of the Mn-doped $YBa_2Cu_3O_{7-\delta}$ (Y-123) system, and Rao *et al* [3] have investigated the specific heat of the Mn-doped $YBa_2Cu_3O_{7-\delta}$ and $GdBa_2Cu_3O_{7-\delta}$ systems.

A recent study by us [16] on a comparison of the effect of Mn on the resistivity of the $YBa_2Cu_3O_{7-\delta}$ and $Y_{0.95}Pr_{0.05}Ba_2Cu_3O_{7-\delta}$ systems has revealed a significant 'electronic effect' for the 0.5% Mn content sample. 'Electronic effect' here refers to either one or both of the following two processes: (1) electron transfer from or to Mn; (2) spectral weight transfer. In fact, aliovalent substitutions may produce electronic effects or simply behave like magnetic or electric scatterers to the excitations of the present system. In the present paper we extend the above type of comparison to make a detailed analysis of the effect of Mn by comparing the thermal transport (thermal conductivity and TEP) of the $YBa_2(Cu_{1-x}Mn_x)_3O_{7-\delta}$ and $GdBa_2(Cu_{1-x}Mn_x)_3O_{7-\delta}$ systems. Thermal conductivity data is used for extracting information on the superconducting state of the Mn-substituted cuprates. TEP, being more sensitive to defects when compared to resistivity data, is considered to extract information about the normal state.

2. Experimental techniques

Samples of the $YBa_2(Cu_{1-x}Mn_x)_3O_{7-\delta}$ and $GdBa_2(Cu_{1-x}Mn_x)_3O_{7-\delta}$ systems in the nominal doping range $0 \leqslant x \leqslant 0.02$ were synthesized following the solid-state reaction route, as described elsewhere [3]. Thermal conductivity (κ) measurements in the range 10–140 K were carried out in a closed-cycle refrigerator, using a direct-pulse technique. Samples were cut to a rectangular parallelepiped shape with typical sizes of $1.5 \times 1.5 \times 5.0$ (mm^3). One end was thermally glued to a copper block (heat sink), and a calibrated chip resistor (100 Ω), which served as a heat source, was glued to the other end. The temperature difference was measured by an E-type differential thermocouple with junctions thermally attached to two well-separated positions along the sample. The temperature difference was controlled to less than 1 K to minimize the heat radiation. The measurements were steady-state experiments. During measurements the sample space was maintained in a good vacuum (better than 10^{-4} Torr). Measurements of the thermoelectric power (S) in the temperature range 10–140 K were performed using a dc pulse technique. The Seebeck voltage was detected using a pair of thin Cu wires electrically connected to the sample with silver paste at the same positions as the junctions of the thermocouple. Stray thermal e.m.f.s were eliminated by applying long current pulses (for about 100 s) to a chip resistor that serves a heater where the pulses appear in an off–on–off sequence. All experiments were performed on a warming cycle at a slow rate
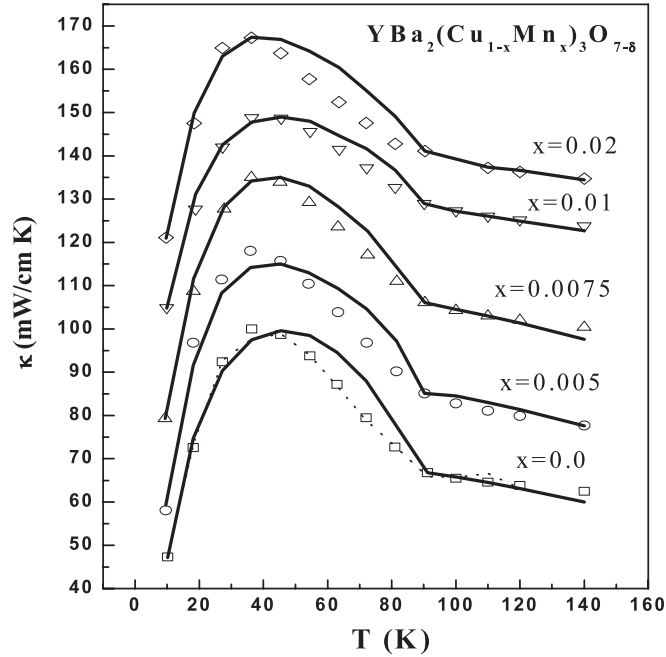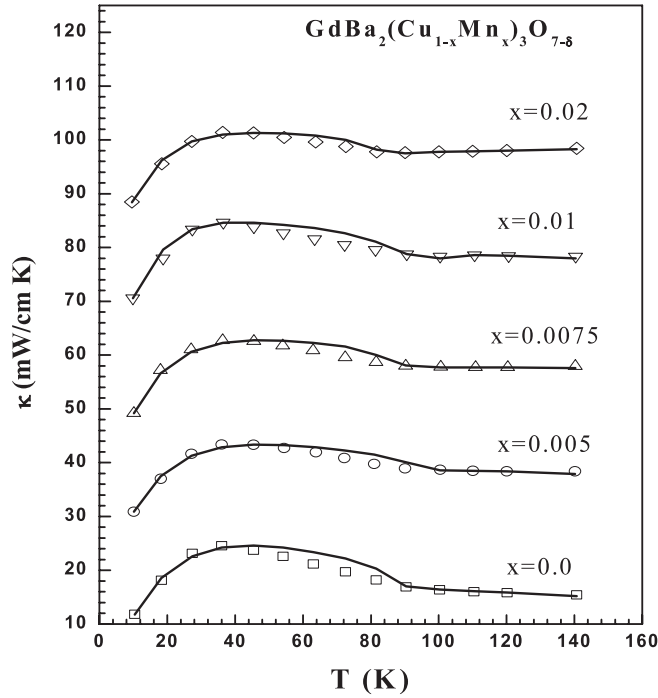
Figure 1. Temperature dependence of thermal conductivity (κ) of $YBa_2(Cu_{1-x}Mn_x)_3O_{7-\delta}$ for $x \leqslant 0.02$. Solid lines show the fitting with the experimental data for $x \leqslant 0.02$. Dashed line is the fitting with the parameter $p = 0.92$.

of $\leqslant 20$ K h^{-1}. The reproducibility of the $S(T)$ and $\kappa(T)$ measurements is better than 2%, while the uncertainty in κ is about 10%, mainly due to error in the determination of sample dimensions.

3. Thermal conductivity

The thermal conductivity of the $YBa_2(Cu_{1-x}Mn_x)_3O_{7-\delta}$ and $GdBa_2(Cu_{1-x}Mn_x)_3O_{7-\delta}$ systems in the temperature range 10–140 K (figures 1 and 2) depicts a hump below their respective T_c values. The hump signifies the occurrence of electron–phonon interaction in the lattice theory of thermal conductivity [17, 18]. In order to analyse the hump structure we consider the peak temperature T_{peak} with the peak value of the thermal conductivity being κ_{peak}. Peak height reduction in the Gd-based cuprates is much faster ($\sim$one fourth) compared to the Y-based samples. Figure 3 depicts the T_{peak} values along with the percentage peak enhancement $E = 100[\frac{[\kappa_{peak} - \kappa(T_C)]}{\kappa(T_C)}]$ with respect to the $\kappa(T_c)$ value. T_{peak} and E vary in a similar fashion for $YBa_2(Cu_{1-x}Mn_x)_3O_{7-\delta}$ with Mn content $\leqslant 0.0075$ and are opposite to each other thereafter, while for $GdBa_2(Cu_{1-x}Mn_x)_3O_{7-\delta}$ the variation in T_{peak} and E is opposite to each other for the entire range of Mn content (0–0.02). The main reason for such different behaviour in the two systems is attributed to the magnetic character of the Gd^{3+} ion vis-à-vis the non-magnetic Y^{3+} ion. Since Mn^{k+} ($k = 2, 3, 4$) also has magnetic character, the $YBa_2(Cu_{1-xo}Mn_{xo})_3O_{7-\delta}$ system will also have an extra magnetic effect for $x_o > 0$. Then it may happen that, for some value of x_o, the doping of Mn in $YBa_2(Cu_{1-x}Mn_x)_3O_{7-\delta}$ leading to $YBa_2(Cu_{1-xo-x}Mn_{xo+x})_3O_{7-\delta}$, and in $GdBa_2Cu_3O_{7-\delta}$ leading to $GdBa_2(Cu_{1-x}Mn_x)_3O_{7-\delta}$, would produce qualitatively similar effects. We indeed find that, for $x_0 = 0.0075$, Mn doping

3

**Figure 2.** Temperature dependence of thermal conductivity (κ) of $GdBa_2(Cu_{1-x}Mn_x)_3O_{7-\delta}$ for $x \leqslant 0.02$. Solid lines show fitting with the experimental data for $x \leqslant 0.02$.

produces qualitatively similar effects in $YBa_2(Cu_{1-xo}Mn_{xo})_3O_{7-\delta}$ and $GdBa_2Cu_3O_{7-\delta}$. In order to clarify this point, in figure 3 we plot the value of $T'_{peak}(x) = T_{peak}(x_0 + x)$ and $E'_{peak}(x) = E_{peak}(x_0 + x)$ (dashed lines) for the Y-based system for $x = 0$–0.01. These values (dashed lines) exhibit similar pattern variations as the corresponding curves for the Gd-based system. In this sense we may argue that doping of Mn in $GdBa_2Cu_3O_{7-\delta}$ is qualitatively similar to doping of Mn in $YBa_2(Cu_{0.9925}Mn_{0.0075})_3O_{7-\delta}$. We emphasize that such similarities hold only for $x \leqslant 0.01$. Moreover, the qualitative difference is quite sharp, at least in the case of the quantity E. In fact, at $x = 0.005$ the difference is about 50%. Figure 3 also depicts that both T_{peak} and E are in general reduced due to Gd for a given Mn content. The only exception is in T_{peak} at $x = 0.02$. For $x > 0$, T_{peak} suffers a maximum reduction of 5.5 K at $x = 0.01$, where values of E for $YBa_2(Cu_{1-x}Mn_x)_3O_{7-\delta}$ and $GdBa_2(Cu_{1-x}Mn_x)_3O_{7-\delta}$ are almost equal.

Let us also consider the thermal conductivity data from the viewpoint of the broadness, ΔT, of the peaks of the observed thermal conductivity of the YMn and GdMn systems. From figures 1 and 2 we find that the value of ΔT for the YMn system is 46.8 K for $x < 0.02$ and 39.4 K for $x = 0.02$. For the GdMn system, the values of ΔT are 45.0, 45.0, 42.1, 37.5 and 38.5 K, respectively, for $x = 0.0, 0.005, 0.0075, 0.01$ and 0.02, which are lower by about 4%, 4%, 10%, 20% and 3% compared to the YMn system. The difference is considerable only for the $x = 0.01$ sample. From table 1 we see that the electron–phonon scattering is quite different for the YMn and GdMn systems. It thus appears that the large difference in the broadness, ΔT, of κ for the $x = 0.01$ sample of the YMn and GdMn systems corresponds to the very different electron–phonon scattering rates.

We now turn to the quantitative details of the thermal conductivity data. From [3] it may be worked out that the resistivities (ρ) of the $YBa_2(Cu_{1-x}Mn_x)_3O_{7-\delta}$ and

4
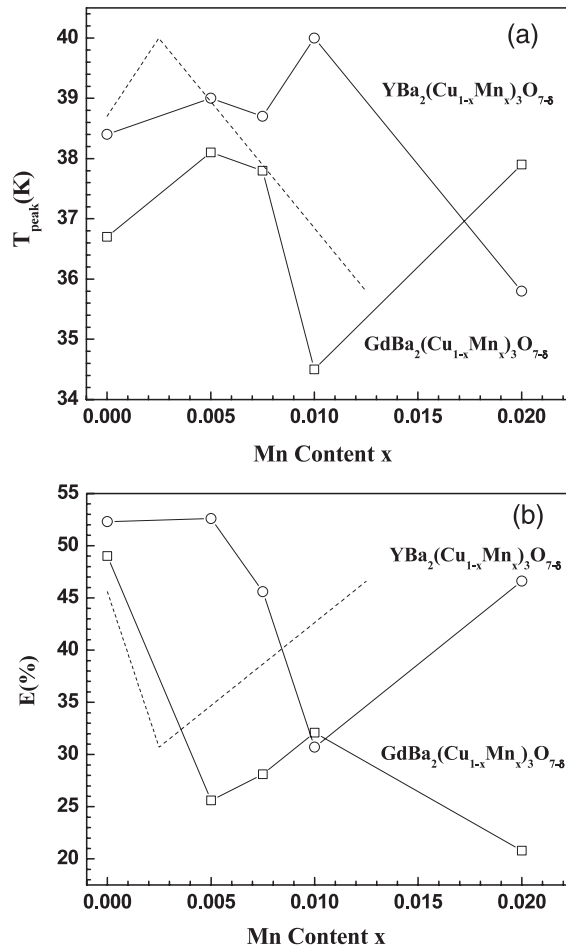
Figure 3. Variation of T_{peak} and E for the $\text{YBa}_2(\text{Cu}_{1-x}\text{Mn}_x)_3\text{O}_{7-\delta}$ and $\text{GdBa}_2(\text{Cu}_{1-x}\text{Mn}_x)_3\text{O}_{7-\delta}$ systems for various Mn content x. Dashed line shows T_{peak} or E with Mn doping with respect to the $\text{YBa}_2(\text{Cu}_{1-0.0075}\text{Mn}_{0.0075})_3\text{O}_{7-\delta}$ system.

$\text{GdBa}_2(\text{Cu}_{1-x}\text{Mn}_x)_3\text{O}_{7-\delta}$ samples are in general much larger than 0.14 mΩ cm. Thus, according to the Wiedemann–Franz law, the electronic contribution to the thermal conductivity will in general be much smaller than $L_0 T/\rho \approx 0.0175$ T. (Here, $L_0 = 2.45 \times 10^{-8}$ W Ω K^{-2} is the Lorentz number.) This magnitude is quite small in comparison to the measured thermal conductivity. Thus, we analyse the observed thermal conductivity in terms of the lattice thermal conductivity only similar to that followed in [17, 18] and unlike Houssa and Ausloos [19], who analysed the thermal conductivity of cuprates in terms of electronic models.

In the lattice model, the thermal conductivity is contributed by a number of processes [17, 18] out of which the following are significant: (1) boundary scattering of phonons; (2) scattering of phonons from point defects; (3) scattering of phonons from the strain field of sheet-like faults; (4) electron–phonon scattering; and (5) phonon–phonon scattering (Umklapp process). We consider these five processes in a way similar to that described by Tewordt and Wolkhausen [17] and by Peacor *et al* [18] to obtain the following expression of

Table 1. Values of parameters A, α, β, γ, θ_D, $2\Delta(0)/k_B T_C$ and U according to the fitting of equation (1) with the thermal conductivity data of $YBa_2(Cu_{1-x}Mn_x)_3O_{7-\delta}$ and $GdBa_2(Cu_{1-x}Mn_x)_3O_{7-\delta}$ for various x. T_c values taken from figures 1 and 2 are also shown here.

Sample	T_c (K)	A (cm K mW^{-1})	α (cm K mW^{-1})	β (cm K mW^{-1})	γ (cm K mW^{-1})	Θ_D (K)	$2\Delta(0)/k_B T_c$	U (cm K mW^{-1})
$YBa_2Cu_3O_{7-\delta}$	91.2	0.09	27.0	1.26	1.89	384.5	5.0	3.7
$YBa_2(Cu_{0.995}Mn_{0.005})_3O_{7-\delta}$	90.3	0.14	16.1	1.96	3.92	396.5	3.7	5.9
$YBa_2(Cu_{0.9925}Mn_{0.0075})_3O_{7-\delta}$	89.9	0.11	22.0	1.54	2.20	393.5	3.7	4.7
$YBa_2(Cu_{0.99}Mn_{0.01})_3O_{7-\delta}$	90.2	0.08	37.6	1.12	1.12	392.5	3.4	2.3
$YBa_2(Cu_{0.98}Mn_{0.02})_3O_{7-\delta}$	86.5	0.10	29.0	1.40	2.95	391.5	3.2	3.2
$GdBa_2Cu_3O_{7-\delta}$	91.8	0.36	105.8	5.09	8.75	383	4.1	12.0
$GdBa_2(Cu_{0.995}Mn_{0.005})_3O_{7-\delta}$	91.8	0.39	113.3	5.47	5.86	393	2.9	5.8
$GdBa_2(Cu_{0.9925}Mn_{0.0075})_3O_{7-\delta}$	90.4	0.62	74.5	8.70	14.29	388	2.6	6.2
$GdBa_2(Cu_{0.99}Mn_{0.01})_3O_{7-\delta}$	89.2	0.53	63.2	7.37	14.74	384	2.3	10.0
$GdBa_2(Cu_{0.98}Mn_{0.02})_3O_{7-\delta}$	86.3	0.85	56.4	11.97	22.22	393	2.2	5.1

the thermal conductivity within a lattice model:

$$\kappa = t^3 \int_0^{\theta_D/T} \frac{u^4 e^u}{(e^u - 1)^2 s(t, u)} \, du \tag{1}$$

where

$$s(t, u) = A + \alpha t^4 u^4 + \beta t^2 u^2 + \gamma t u g(u, y(t)) + U t^4 u^2 \tag{2}$$

with $t = \frac{T}{T_c}$ as the reduced temperature, and $y(t) = \frac{\Delta(t)}{k_B T_c t}$.

Here, $2\Delta(t)$ is the superconducting energy gap at the reduced temperature t. In the present study, for $\Delta(t)$ we have used the BCS-like t-dependence:

$$\Delta(t) = \Delta(0) \tanh(b\{t^{-1} - 1\}^{1/2}). \tag{3}$$

In fact, this t-dependence has been used by many authors in the high-T_c literature [19, 20], with the values of b lying between 1.7 and 2.2. Specifically, we have taken $b = 2.0$ in the present analysis. In equation (2), A is a constant, which is proportional to the boundary scattering. The parameters α, β, γ and U represent, to within a constant, the scattering rates of phonons with, respectively, the point defects, sheet-like faults, electrons and phonons. The function $g(u, y(t))$ in equation (2) is defined, for example, by equation (8) of Tewordt and Wolkhausen [17]. $g(u, y)$ decreases with increasing y in the interval $0 \leqslant u \leqslant 2y$. The decrement of $g(u, y)$ corresponds to the decrease in superconducting quasi-particles. At $u = 2y$, $g(u, y)$ shows a step signifying the onset of the excitation of pairs of quasi-particles for $u \geqslant 2y$. We emphasize that it is the structure of $g(u, y)$ which causes the hump in κ between $T = 0$ and $T = T_c$ (figures 1 and 2).

We have obtained values of the parameters A, α, β, γ and U for different Mn contents by fitting the experimentally observed thermal conductivity with equation (1) for both YBa$_2$(Cu$_{1-x}$Mn$_x$)$_3$O$_{7-\delta}$ and GdBa$_2$(Cu$_{1-x}$Mn$_x$)$_3$O$_{7-\delta}$ (table 1). The solid lines in figures 1 and 2 refer to the fitting of equation (1) with experimental data for various x. In general, the fitting is poor between 36 K and T_c except for the $x = 0.02$ sample of GdBa$_2$(Cu$_{1-x}$Mn$_x$)$_3$O$_{7-\delta}$. We attribute it to the highly asymmetric nature of the data about T_{peak}, while the theory used by us (equation 1) leads to an almost symmetric variation of κ about T_{peak} when the peak height (E) is large. In fact, for low E the hump structure tends to be symmetric. This is clear from the figure 2 of Peacor *et al* [18] and also from the figure 2 of Tewordt and Wolkhausen [17]. Since our data, except for the $x = 0.02$ sample of the Gd-based system, correspond to large values of E, it is not possible to bring asymmetry in the hump structure within the model of equations (1)–(3). One source for the symmetry of κ about T_{peak} is the t-dependence of $\Delta(t)$ of equation (3). We have found that when the square-root part $(t^{-1} - 1)^{1/2}$ of equation (3) is replaced by $(t^{-1} - 1)^p$ then the agreement of experimental data with the theory becomes better for $p > 1/2$. For example, for the $x = 0$ sample of the Y-based system the agreement between theory and experimental becomes quite good for $p = 0.92$ and $2\Delta/k_B T_c = 7.0$. The value of A is slightly decreased to 0.08 cm K mW^{-1}, α is increased to 31.5 cm K mW^{-1}, β is decreased to 1.15 cm K mW^{-1} and γ is considerably enhanced to 2.71. For cuprates these values of p and $2\Delta/k_B T_c$ are quite reasonable. We emphasize that the discrepancy in the fitting of experimental data with equation (1) is present for all the samples. However, a relative study of the effects of different Mn contents on the thermal conductivity of GdBa$_2$(Cu$_{1-x}$Mn$_x$)$_3$O$_{7-\delta}$ is still expected to be useful. Further, we notice from table 1 that $2\Delta(0)$, although different from that for a BCS superconductor ($= 3.5 k_B T_c$), is finite for all values of Mn content. Thus the thermal conductivity data does not support gapless superconductivity.

We now consider the relative values of the parameters A, α, β, γ and U. It is interesting to note that, for the YBa$_2$(Cu$_{1-x}$Mn$_x$)$_3$O$_{7-\delta}$ system, A, β and γ follow the same qualitative
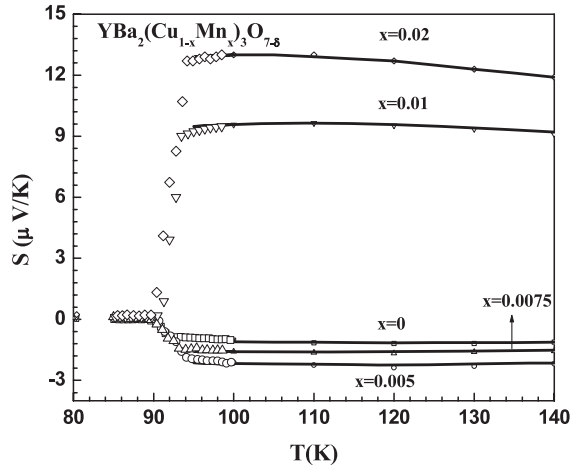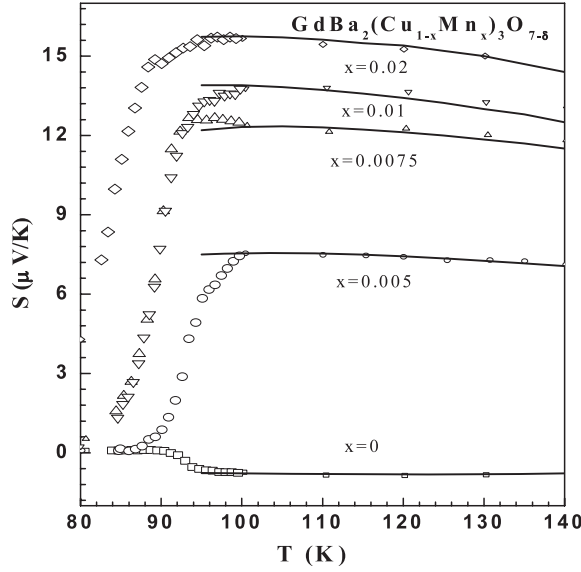
Figure 4. Temperature dependence of thermoelectric power (S) of $YBa_2(Cu_{1-x}Mn_x)_3O_{7-\delta}$ for $x \leqslant 0.02$ up to 200 K. Solid lines show fitting with the experimental data for $x \leqslant 0.02$.

variation as E, whereas the variation of α is opposite to E. Thus in $YBa_2(Cu_{1-x}Mn_x)_3O_{7-\delta}$ the hump structure in κ appears to be related independently to the boundary scattering, sheet-like faults and electron–phonon interaction. In the case of $GdBa_2(Cu_{1-x}Mn_x)_3O_{7-\delta}$ superconductor, only the phonon–phonon interaction term U appears to relate to E completely, although γ also shows a relation to E up to $x = 0.01$. Thus, in this system the boundary scattering, point defects and sheet-like faults combine together to drive the hump structure.

Let us now examine the role of Mn from the superconductivity viewpoint. From table 1 we see that the gap ratio $2\Delta(0)/k_B T_c$ changes significantly up to $x = 0.005$ substitution of Mn in both Y- and Gd-based systems. Further doping ($x > 0.005$) has little effect on $2\Delta(0)/k_B T_c$. If we interpret the significant change in the gap ratio by $x = 0.005$ Mn in $GdBa_2(Cu_{1-x}Mn_x)_3O_{7-\delta}$ due to the magnetic effect of Gd ions, we should expect, in view of the proceeding similarity of $GdBa_2Cu_3O_{7-\delta}$ with $YBa_2(Cu_{1-x}Mn_x)_3O_{7-\delta}$, a significant change in $2\Delta(0)/k_B T_c$ above $x = 0.0075$ in $YBa_2(Cu_{1-x}Mn_x)_3O_{7-\delta}$ which, however, is not the case (cf table 1). This means that the magnetic effect (due to Gd ions or Mn ions) does not play a significant role in the superconducting pairing process. We expect a similar possibility on the basis of the T_c values too. This is because the decrease in T_c by $x = 0.005$ Mn with respect to the $x = 0$ sample and that by $x = 0.01$ Mn with respect to the $x = 0.0075$ sample are similar. The decrements in T_c in these two stages would have been visibly different if the magnetic effect had any role to play in their T_c degradation. Potential scattering is a possible source of T_c degradation for the cuprates, being d-wave superconductors [21]. However, if potential scattering had been completely responsible for the T_c degradation, the decrease in T_c with Mn should have been monotonic. The non-monotonic decrease in T_c with Mn rules out the possibility of T_c degradation due to potential scattering only. Thus, along with potential scattering, some other mechanism is also operating in T_c degradation. The situation for cuprates suggest that it is an 'electronic effect'. Whether it is electron transfer or spectral weight transfer or both will be considered in the next section.

4. Thermoelectric power

The thermoelectric powers, $S(T)$, of Mn-doped Y- and Gd-based systems are shown in figures 4 and 5, respectively, for the temperature range 95–140 K and are qualitatively similar to that
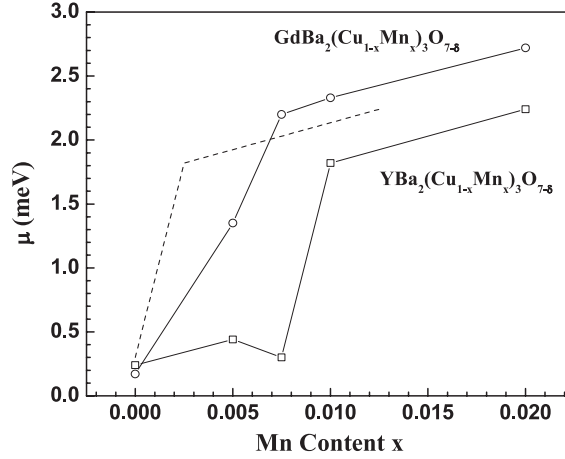
Figure 5. Temperature dependence of thermoelectric power (S) of $GdBa_2(Cu_{1-x}Mn_x)_3O_{7-\delta}$ for $x \leqslant 0.02$ up to 200 K. Solid lines show fitting with the experimental data for $x \leqslant 0.02$.

observed earlier for various $YBa_2Cu_3O_{7-\delta}$ superconductors [5, 7]. Figures 4 and 5 depict $S(T)$ of $YBa_2Cu_3O_{7-\delta}$ and $GdBa_2Cu_3O_{7-\delta}$ to be electron-like in nature and much closer quantitatively. On the other hand, Mn content of $x = 0.01$ in $YBa_2(Cu_{1-x}Mn_x)_3O_{7-\delta}$ and $x = 0.005$ in $GdBa_2(Cu_{1-x}Mn_x)_3O_{7-\delta}$ changes the nature of the TEP from electron-like to hole-like. Also, the change in magnitude of S with $x = 0.01$ Mn in $YBa_2(Cu_{1-x}Mn_x)_3O_{7-\delta}$ and $x = 0.005$ Mn in $GdBa_2(Cu_{1-x}Mn_x)_3O_{7-\delta}$ is of one order. Thus, it is the $YBa_2(Cu_{1-0.0075}Mn_{0.0075})_3O_{7-\delta}$ system which shows a similar behaviour of TEP with (further) Mn doping to the system $GdBa_2Cu_3O_{7-\delta}$. This means that, both from the qualitative and quantitative viewpoints, the TEP of $YBa_2(Cu_{1-0.0075}Mn_{0.0075})_3O_{7-\delta}$ and $GdBa_2Cu_3O_{7-\delta}$ systems are similar, which substantiates the inference drawn on the basis of the thermal conductivity analysis in section 3. The behaviour of S in cuprate superconductors has been considered on various bases, namely the narrow band picture [5], resonance valence bond theory [22] and on the van Hove singularity [23]. In the present case, we have analysed the data with the narrow-band picture. In fact, it has been shown that the narrow-band picture explains the resistivity and Hall effect of the cuprate superconductors as well [5]. The narrow-band picture describes S in terms of three parameters, namely n, W_D and W_σ, where n is the band filling, W_D is the total effective band width of the electronic states (usually higher than 1000 K) and W_σ denotes the effective width of an energy interval for electronic conduction such that $W_\sigma < W_D$. We may recast the expression for S obtained in [5] in the form

$$S = \frac{k_B}{e \sinh W_\sigma^*} \left[W_\sigma^* \sinh \mu^* + \mu^*(\cosh \mu^* + \exp W_\sigma^*) \right.$$
$$\left. + (\cosh \mu^* + \cosh W_\sigma^*) \ln \frac{1 + e^{W_\sigma^* - \mu^*}}{1 + e^{W_\sigma^* + \mu^*}} \right] \tag{4}$$

where

$$\mu^* = \ln[\sinh(n W_D^*) / \sinh(W_D^* - n W_D^*)] \tag{5}$$

Figure 6.   Variation of the chemical potential μ with various Mn contents of $YBa_2(Cu_{1-x}Mn_x)_3O_{7-\delta}$ and $GdBa_2(Cu_{1-x}Mn_x)_3O_{7-\delta}$ samples.   Dashed line shows μ with Mn doping with respect to the $YBa_2(Cu_{1-0.0075}Mn_{0.0075})_3O_{7-\delta}$ system.

and

$$W_\sigma^* = \frac{W_\sigma}{2k_BT} \tag{6}$$

with

$$W_D^* = W_D/2k_BT. \tag{7}$$

In equation (4), e is the electronic charge of a carrier and k_B is the Boltzmann constant. We now estimate the chemical potential μ from the narrow band picture for the $YBa_2(Cu_{1-x}Mn_x)_3O_{7-\delta}$ and $GdBa_2(Cu_{1-x}Mn_x)_3O_{7-\delta}$ systems. The chemical potential is given by [5]

$$\mu = \mu^* k_BT. \tag{8}$$

According to equations (5) and (7), μ appears to be dependent on T for given values of n and W_D. In order to avoid the problem, we notice that, for $2k_BT \ll W_D$, $\mu^* \to (2n-1)W_D/2k_BT$. When this is so, $\mu = (2n-1)W_D$ becomes independent of T. Thus, for low T we can estimate values of μ for different samples in the framework of the narrow-band picture. This in fact explains why we have considered the TEP in figures 4 and 5 up to $T = 140$ K only.

We have fitted the experimental data of TEP with equation (4), and this is shown by solid lines in figures 4 and 5. The chemical potential μ obtained from such fittings is shown in figure 6. Comparing figures 4 and 5 with figure 6, μ is found to increase with $S(T)$ in the temperature range 100–140 K. Similar conclusions may be drawn by comparing the figures 10–12 of Gasumyants *et al* [5] and by using the formula $\mu = (2n-1)W_D$. Although such a comparison with $\mu = (2n-1)W_D$ is only roughly true because Gasumyants *et al* [5] have carried out fittings up to higher values of T, where $\mu = (2n-1)W_D$ is not exactly valid, the increment of μ with $S(T)$ will be correct qualitatively. We emphasize that, in the Fermi gas model, the Fermi energy varies inversely with $S(T)$. As in the case of the thermal conductivity, we have also plotted the quantities $\mu'(x) = \mu(x_0 + x)$ for the $YBa_2(Cu_{1-x}Mn_x)_3O_{7-\delta}$ samples. This plot is shown by dashed lines in figure 6 and is qualitatively similar to the behaviour of μ for the $GdBa_2(Cu_{1-x}Mn_x)_3O_{7-\delta}$ samples. Thus the fitted values of the chemical potential provide yet another support to the point that Mn doping with respect

to the $YBa_2(Cu_{1-0.0075}Mn_{0.0075})_3O_{7-\delta}$ and $GdBa_2Cu_3O_{7-\delta}$ samples possess similar thermal behaviours.

From the above, we have seen that, on the basis of the chemical potential, the considered samples are divided into two categories, namely low-μ samples ($\mu \leqslant 0.44$ meV) ($YMn_{0.0}$, $YMn_{0.005}$, $YMn_{0.0075}$ and $GdMn_{0.0}$) and high-μ samples ($\mu \geqslant 1.35$ meV) ($YMn_{0.01}$, $YMn_{0.02}$ and $GdMn_x$ for all $x > 0$). Since the cuprate systems are not rigid band systems, doping (by Mn or other elements) also causes spectral weight transfer [24]. Thus, while changing Mn content to go from the low-μ to the high-μ samples, we expect a large spectral weight transfer in the system. In fact, the narrow-band approach considered here for the analysis of the S data is in essence phenomenological in nature. So, a large change (about five times) in μ is a phenomenological illustration of the spectral weight transfer in these cuprate systems. Thus we may say that, beyond $x = 0.0075$ Mn in the superconductor $YBa_2(Cu_{1-x}Mn_x)_3O_{7-\delta}$, there are electronic effects due to Mn.

5. Conclusions

Thermal conductivity $\kappa(T)$ and thermoelectric power $S(T)$ studies of the Mn-doped Y- and Gd-based superconducting cuprates synthesized under similar conditions are presented here. The qualitative behaviour of these quantities below and above T_c, as characterized by relative variations in $T_{peak}(x)$, $E(x)$ and $S(x)$, suggest that Mn plays different roles for x above and below 0.0075 in the $YBa_2(Cu_{1-x}Mn_x)_3O_{7-\delta}$ system. In fact, up to $x = 0.0075$, Mn plays the role of magnetic ions between CuO_2 layers, similar to that of Gd in $GdBa_2(Cu_{1-x}Mn_x)_3O_{7-\delta}$. On the other hand, beyond $x = 0.0075$, Mn causes drastic changes in the $YBa_2(Cu_{1-0.0075}Mn_{0.0075})_3O_{7-\delta}$ system which are sharp in TEP but not in T_{peak} and E.

The main point of the study is that Mn requires a magnetic background to produce a significant effect in the cuprate superconductors. In $YBa_2(Cu_{1-x}Mn_x)_3O_{7-\delta}$, there is no magnetic background up to $x = 0.0075$, but for $x > 0.0075$ the magnetic background is provided by the Mn content itself. In $GdBa_2(Cu_{1-x}Mn_x)_3O_{7-\delta}$ the magnetic background is provided by the Gd ions and is operative even for the smaller Mn content ($x = 0.005$). We have seen in a recent study [16] that, when 5.0% Pr is substituted for Y in $Y_{0.95}Pr_{0.05}Ba_2(Cu_{1-x}Mn_x)_3O_{7-\delta}$, the effect of Mn appears to reflect the presence of the magnetic background. In fact, with 5.0% Pr, Mn content of $x = 0.005$ provides a significant effect in resistivity and ac susceptibility. In this case, the Pr provides the required magnetic background. This role of Mn could not be studied in the earlier studies by other authors in the Mn-substituted Y-based cuprates because, in most of these studies, samples with such low contents as $x = 0.005$ and 0.0075 are not considered.

References

[1] Yang J, Zhang B, Zhou H, Ding Y, Jin L, Ye C, Yang Y, Zha Y and Yuan W 1989 *Solid State Commun.* **70** 919
[2] Saini N L, Garg K B, Rajagopal H and Sequeira A 1992 *Solid State Commun.* **82** 895

[3] Rao A, Radheshyam S, Das A, Gahtori B, Agarwal S K, Lin Y K, Sivakumar K M and Kuo Y K 2006 *J. Phys.: Condens. Matter* **18** 2955
[4] Dhingra I, Kashyap S C and Das B K 1994 *J. Mater. Res.* **9** 2771
[5] Gasumyants V E, Kaidanov V I and Vladimirskaya E V 1995 *Physica* C **248** 255
[6] Samuel E I, Seshu Bai V, Sivakumar K M and Ganesan V 1999 *Phys. Rev.* B **59** 7178
[7] Samuel E I, Seshu Bai V, Harish Kumar N and Malik S K 2001 *Supercond. Sci. Technol.* **14** 429
[8] Tallon J L, Cooper J R, de Silva P S, Williams G V M and Loram J W 1995 *Phys. Rev. Lett.* **75** 4114
[9] Zhang Q M, Xu X S, Ying X N, Li A, Qiu Q, Wang Y N, Xu G J and Zhang Y H 2000 *Physica* C **337** 277
[10] Honma T, Hor P H, Hsieh H H and Tanimoto M 2004 *Phys. Rev.* B **70** 214517
[11] Suleiman B M, Börjesson L and Berastegui P 1996 *Phys. Rev.* B **53** 5901
[12] House M, Aisles M and Clots R 1997 *Phys. Rev.* B **56** 6226
[13] Williams R K, Martin P M and Scarborough J O 1999 *Phys. Rev.* B **59** 13639
[14] Loram J W, Mirza K A, Freeman P F and Tallon J J 1991 *Supercond. Sci. Technol.* **4** S184
[15] Sisson D L, Doettinger S G, Kapitulnik A, Liang R, Bonn D A and Hardy W N 2000 *Phys. Rev.* B **61** 3604
[16] Gahtori B, Lal R, Ahsan M A H, Shyam R, Rao A and Agarwal S K 2006 *Physica* C **449** 128
[17] Tewordt L and Wolkhausen Th 1989 *Solid State Commun.* **70** 839
[18] Peacor S D, Richardson R A, Nori F and Uher C 1991 *Phys. Rev.* B **44** 9508
[19] Houssa M and Ausloos M 1996 *Physica* C **257** 321
[20] Yu R C, Salamon M B, Lu J P and Lee W C 1992 *Phys. Rev. Lett.* **69** 1431
[21] Tsuei C C, Kirtley J R, Chi C C, Lock See Y-J, Gupta A, Shaw T, Sun J Z and Ketchen M B 1994 *Phys. Rev. Lett.* **73** 593
[22] Nagaosa N and Lee P A 1990 *Phys. Rev. Lett.* **64** 2450
[23] Newns D M, Tsuei C C, Huebener R P, van Bentum P J M, Pattnaik P C and Chi C C 1994 *Phys. Rev. Lett.* **73** 1695
[24] Veenendaal van M A and Sawatzky G A 1994 *Phys. Rev.* B **49** 1407